ACADEMIC PRESS

Available online at www.sciencedirect.com
SCIENCE DIRECT®

Journal of Catalysis 218 (2003) 296–306

JOURNAL OF CATALYSIS

www.elsevier.com/locate/jcat

Oxidative conversion of propane over lithium-promoted magnesia catalyst I. Kinetics and mechanism

L. Leveles,[a] K. Seshan,[a] J.A. Lercher,[b] and L. Lefferts [a,*]

[a] *Faculty of Chemical Technology, University of Twente, Postbus 217, 7500 AE, Enschede, The Netherlands*
[b] *Institute for Chemical Technology, Department of Chemistry, Technische Universität München, Lichtenbergstrasse 4, D-85747 Garching, Germany*

Received 9 October 2002; revised 26 February 2003; accepted 7 March 2003

Abstract

Oxidative conversion of lower alkanes over lithium-promoted magnesia catalysts offers a viable alternative for propene and ethene production. The catalytic performance of propane oxidative dehydrogenation and cracking shows yields up to 50% of olefin (propene and ethene). The reaction kinetics were studied by means of variation of the partial pressures of the reactants as well as by addition of product species to the reaction mixture. The observations can be qualitatively explained with a mechanism including activation of propane on the catalyst generating propyl radicals that undergo a radical-chain mechanism in the gas phase. Alkane activation is rate determining. Oxygen has two functions in the mechanism. First, the presence of small amounts of oxygen influences the radical gas-phase chemistry significantly because the type and concentration of chain propagator radicals are greatly increased. At higher oxygen partial pressures the radical chemistry is only slightly influenced by the increasing oxygen concentration. The second function of oxygen is to facilitate the removal of hydrogen from the surface OH^- species that are formed during the activation of propane on the catalyst. Carbon dioxide has a strong inhibiting effect on the reaction without changing the product distribution, due to strong adsorption on the site that activates propane.

Keywords: Alkanes oxidative dehydrogenation; Olefin production; Propylene; Ethylene; Li/MgO; Radical surface interactions

1. Introduction

An increased olefin demand (especially C_2–C_4 olefins) is predicted for the coming years [1,2]; consequently industry is seeking alternative routes for the production of lower olefins, as the present production capacity will not meet the needs. In Western Europe propene demand is predicted to grow faster than that for ethene (3.7 vs. 2.4%) in the coming years [3]. The major source of propene currently is steam cracking, which maximizes ethene yield, and consequently, propene production from this source will barely match the consumption. FCC and catalytic dehydrogenation can be industrial alternatives to meet the shortfall of propene production. In the FCC plant propene is produced as a by-product; thus, FCC cannot be used as a dedicated propene production process. The difficulties in carrying out dehydrogenation of alkanes are diverse and are discussed in great detail elsewhere [4]. The main problems in the classical dehydrogenation process are the low conversion caused by thermodynamic constraints and coking. *Oxidative dehydrogenation* (ODH) can be a viable route for the production of olefins as the presence of oxygen counteracts the thermodynamic limitation and prevents coking. While this has been recognized for a long time, an industrially applicable process has not been developed, because secondary oxidation of olefins to carbon oxides is very significant on most materials [5–7]. Thus, the yields of olefins remained under 30%, unsatisfactory for commercial application [8]. Among many other catalysts, vanadia on magnesia support was the most studied because of its high activity [6].

Recently, oxidative conversion of LPG has been reported over Li–Dy–Cl–MgO catalysts: yields of olefins (mixture of butenes, propene, and ethene) as high as 50% were obtained [9,10]. While ethane oxidative dehydrogenation and methane oxidative coupling have been studied extensively over alkali-promoted magnesia [11–14], studies of propane oxidative dehydrogenation over these materials are limited [15,16]. In our recent study [17] oxidative conversion of propane and *n*-butane gave yields of olefins in the range

* Corresponding author.
E-mail address: l.lefferts@ct.utwente.nl (L. Lefferts).

0021-9517/03/$ – see front matter
doi:10.1016/S0021-9517(03)00112-X

of 50%. Propene and ethene were the major olefin products when propane was used as feed. The ratio of propene to ethene was higher compared to steam cracking at similar conversions, implying a strategic advantage for meeting future increased propene demand. From the catalysts reported by Landau et al. (e.g., Li–Cl–Dy–Mg–O) we have shown that lithium was the only essential ingredient for a well-performing catalyst, thus providing a Cl-free oxidation catalyst [17]. Cl^- addition gave only marginal improvements in olefin yields, but induced stability problems. A simplified catalyst system Li/Dy/MgO works equally efficiently. The role of each component in this catalyst has also been discussed in detail earlier [17].

In this paper (part I) we report a detailed study on the reaction kinetics of propane and propene oxidation in the presence of oxygen over Li/Dy/MgO catalysts and the reaction mechanism of propene oxidative conversion will be proposed based mainly on the kinetic measurements. In the subsequent paper (part II) we aim to characterize the active sites of Li-promoted magnesia where the propane activation takes place; and we will discuss the role of Li in the active site.

2. Experimental

The catalyst was prepared by wet impregnation using an aqueous solution of $LiNO_3$ and a mixture of MgO (obtained by calcining $Mg(OH)_2$ at 700 °C for 3 h) and Dy_2O_3 powder with the following target composition of the catalyst: 85 wt% MgO, 7.7 wt% Li_2O, and 7.3 wt% Dy_2O_3. The impregnation step was followed by drying and calcination in air at 750 °C. Catalyst preparation, characterization, and catalytic performance measurements are described elsewhere in more detail [17].

Reaction rates were determined under differential conditions at 600 °C in a kinetic setup employing a quartz microreactor (internal diameter: 4 mm) with a Varian 3800 GC on-line. A catalyst bed of 200 mg catalyst was placed in the microreactor taking up a volume of 250 µl. Two quartz bars with 3 mm diameter were inserted upstream and downstream of the catalyst bed to take up most of the free volume. Thermocouples in quartz sleeves were placed above and below the catalyst bed to measure temperature. The feed for typical measurements consisted of 28% propane, 14% oxygen, 2% carbon dioxide, and balance helium. When the kinetics of propene conversion was measured the typical feed consisted of 28% propene, 7% oxygen, and 1% carbon dioxide. Carbon dioxide has been introduced to the feed in order to achieve a constant CO_2 concentration over the whole catalyst bed, as CO_2 has a strong inhibiting effect upon the reaction (for further details see Section 3). The total flow rate was 100 ml/min unless stated otherwise. Propane conversion was less than 10% and oxygen conversions were lower than 15% in all cases unless otherwise noted. Maximum adiabatic temperature increase was calculated to be 5 K. During experiments ΔT measured across the across the catalyst bed was about 3 K. The carbon balance was within ±3% in all experiments where propane conversion was lower than 10%.

Reaction rates were calculated as mole product formed per second per gram of catalyst ($\mathrm{mol\,s^{-1}\,g^{-1}}$). When measurements were done in the absence of a catalyst, rates were calculated in terms of mole product formed per second per milliliter reactor volume ($\mathrm{mol\,s^{-1}\,ml^{-1}}$). All rates were expressed in terms of reactor volume ($\mathrm{mol\,s^{-1}\,ml^{-1}}$) when rates obtained with catalyst were compared to rates measured in the absence of catalyst, under identical temperature, partial pressure, and flow rate conditions.

Mass transfer and heat transfer limitations were evaluated by calculation. The criteria suggested by Mears indicated the absence of mass- and heat-transfer limitations [18,19].

3. Results

3.1. Influence of temperature on catalytic activity and selectivity

The influence of temperature on the catalytic performance of the Li/MgO catalyst was studied in order to find the optimum temperature interval for the propane conversion reaction. Fig. 1 shows how the selectivities and propane conversion evolve with temperature over 7 wt% Li_2O-promoted magnesia catalyst under constant space velocity. Propene was the main product over the whole temperature range except at 700 °C. The selectivity to ethene continuously increased and above 650 °C it became larger than selectivity to propene. Both the selectivities to CO and CO_2 decreased between 500 and 600 °C, while between 600 and 700 °C they remained fairly constant. Methane selectivity increased continuously.

The above selectivity data were obtained at differing conversion levels. Fig. 2 shows the variation in selectivity of the various products with the level of conversion, measured at 600 °C. It is obvious that selectivities vary only marginally

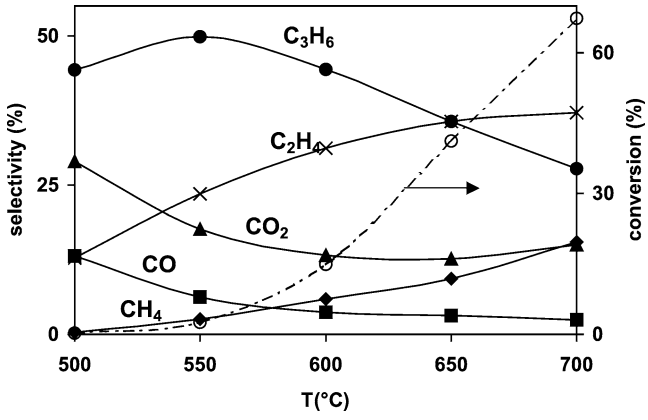

Fig. 1. Conversion of propane and selectivities for various products vs temperature over Li/MgO catalysts. Conditions: 10% propane and 8% oxygen in He; total flow, 10 ml/min; 100 mg catalyst.

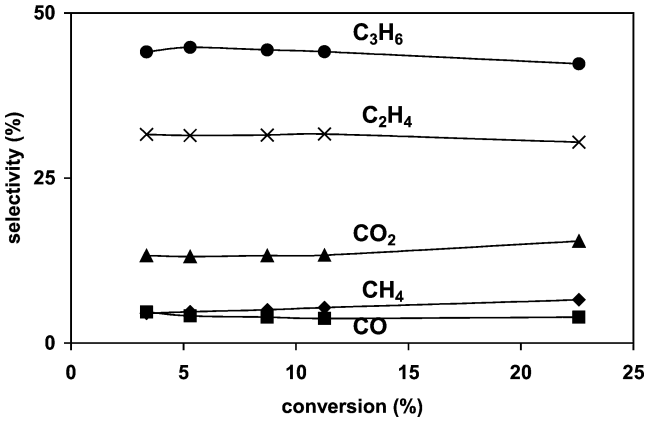

Fig. 2. Selectivities for various products vs propane conversion at 600 °C over Li/MgO catalysts. Conditions: 10% propane and 8% oxygen in He; total flow, 4–80 ml/min; 100 mg catalyst.

with the level of conversion, which is characteristic for all Li-promoted magnesia catalysts. A temperature of 600 °C was chosen for detailed measurement of the kinetics for the Li/Dy/MgO catalyst.

3.2. Propane partial pressure variation

Rates of formation of products varied linearly with propane partial pressure in the range of 0–0.3 bar (Fig. 3). This indicates a first-order reaction, where propane participates in the rate-determining step. Above 0.3 bar the rate of formation of propene, ethene, and methane showed an exponential increase, while the rate of formation of CO and hydrogen continued to vary linearly.

3.3. Oxygen partial pressure variation

The rates of formation of products appear to follow a complex pattern with respect to the oxygen partial pressure (Fig. 4). The rates of formation of propene, ethene, and methane increased steeply at very low oxygen partial pressures, i.e., when increasing oxygen partial pressure from 0 to 5 mbar. It is interesting to note that in the absence of oxygen the molar rates of formation of propene, ethene, and methane are nearly equal. Increasing oxygen in the feed from 0 to 5 mbar maintains this 1:1:1 ratio. Further increase of oxygen content in the feed influenced differently the rates of formation of the different products. Propene continued to increase linearly with oxygen partial pressure while ethene remained constant. Rate of methane formation declined with oxygen partial pressure, while at the same time the formation rate of CO increased. By power-law fit of these data it was calculated that the formation rate of CO has an apparent order of 0.5 in oxygen partial pressure.

It is important to note that the sum of production rates of CH_4 and CO equals the formation rate of ethene independent of the partial pressures of both propane and oxygen. This fact seems to indicate that a common C_1 intermediate leads to formation of CH_4 and CO.

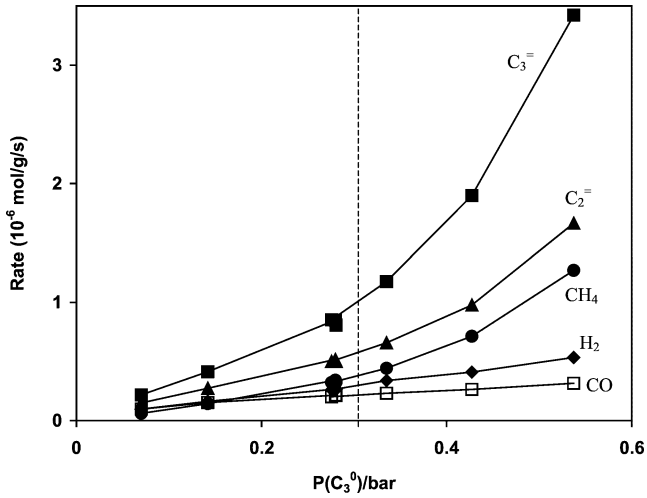

Fig. 3. Rates of formation vs propane ($C_3{}^0$) partial pressure over the catalyst. Conditions: $P(CO_2)$, 20 mbar; $P(O_2)$, 140 mbar; T, 600 °C; total flow, 100 ml/min; 200 mg catalyst.

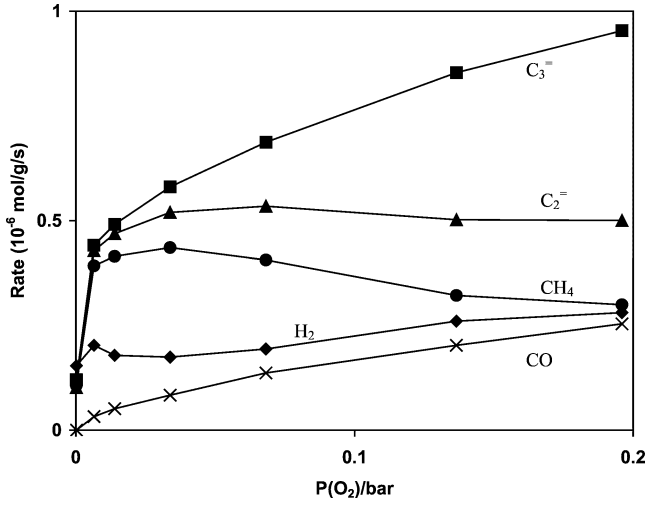

Fig. 4. Rates of formation over the catalyst vs oxygen partial pressure. Conditions: $P(CO_2)$, 20 mbar; $P(C_3H_8)$, 280 mbar; T, 600 °C; total flow, 100 ml/min; 200 mg catalyst.

3.4. Gas-phase reactions

The reaction kinetics of propane conversion was also evaluated in an empty reactor in order to assess the extent to which gas-phase homogeneous reactions influence the conversion of propane. Propane and oxygen partial pressures have been varied in a manner similar to experiments with catalyst present in the reactor. Care has been taken to avoid any Li contamination of the quartz reactor.

When the propane partial pressure was varied during reaction in the empty reactor, the formation rates for all products increased exponentially (Fig. 5). The apparent reaction order increases with propane partial pressure. Formation of CO and H_2 was not detectable below 0.2 bar of propane. Reaction rates varied in a similar fashion with oxygen partial pressure as in the presence of catalyst (Fig. 6). In both cases

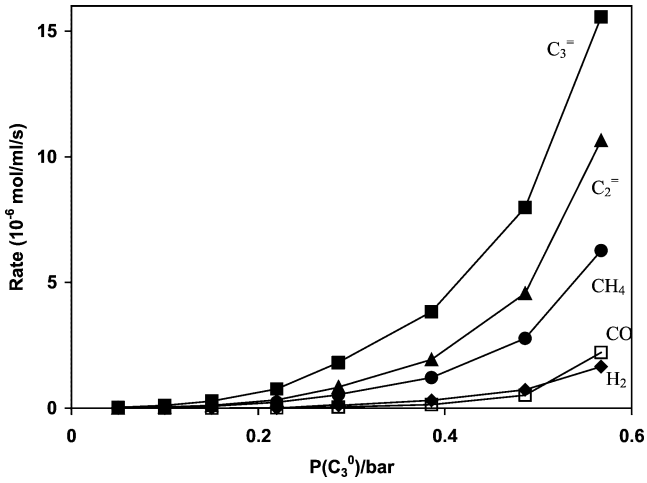

Fig. 5. Formation rates in the empty reactor vs propane partial pressure. Conditions: $P(CO_2)$, 20 mbar; $P(O_2)$, 140 mbar; T, 600 °C; total flow, 100 ml/min; 250 µl cylindrical empty volume.

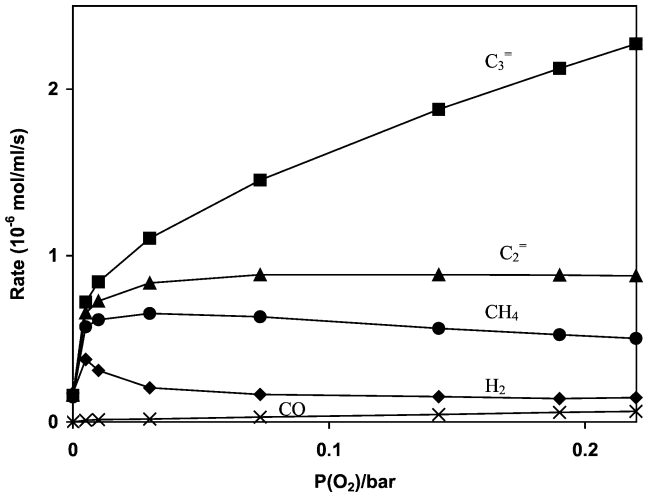

Fig. 6. Formation rates as a function of oxygen partial pressure in the empty reactor. Conditions: $P(CO_2)$, 20 mbar; $P(C_3H_8)$, 280 mbar; T, 600 °C; total flow, 100 ml/min; 250 µl cylindrical empty volume.

a sharp increase at low oxygen pressures was observed. Hydrogen was also formed with a comparable rate. However, the rate of formation of CO was four times lower than that in the presence of catalyst. In the case of the empty reactor the sum of the CO and CH_4 formation rates is not equal to the ethene formation rate (Fig. 6).

The conversion increased linearly with residence time when catalyst was present. In the empty reactor conversion increased exponentially and followed a sigmoidal curve at high residence time due to the exhaustion of oxygen (Fig. 7). At residence times lower than 0.5 s conversion with the catalyst bed was higher, while at higher residence times (> 0.5 s) conversion in the empty reactor was higher than that over the catalyst bed. It must be noted, however, that this experiment was not attempted to be confined to differential conditions and CO_2 was not added to the reaction feed, unlike in all other measurements reported in this paper. The typical residence time for standard conditions of 28% propane, 14% oxygen, 2% CO_2, and balance helium with 100 ml/min total flow rate at 600 °C was 0.15 s in the empty reactor and 0.06 s when the catalyst was present.

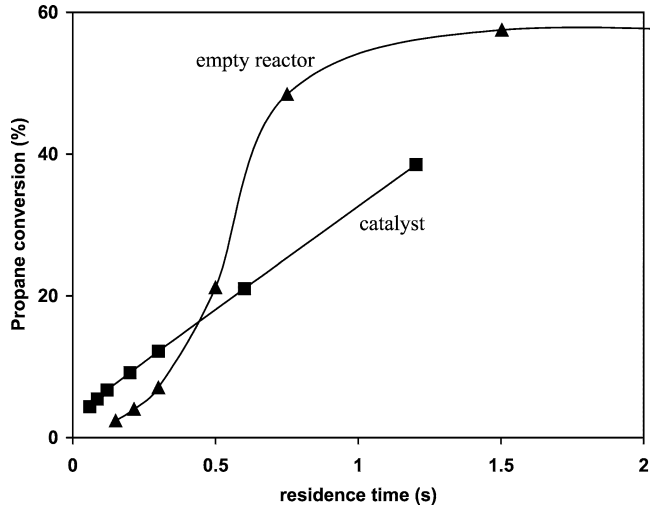

Fig. 7. Conversion of propane vs residence time with and without the catalyst bed. Conditions: $P(C_3H_8)$, 280 mbar; $P(O_2)$, 140 mbar; T, 600 °C; total flow, 5–100 ml/min; 250 µl cylindrical empty volume with and without 200 mg catalyst.

The postcatalytic void downstream of the catalyst bed was increased by the same volume as the volume of the catalyst bed (e.g., 250 µl) by pulling the inserted quartz bar away from the catalyst bed. This change caused a 25% increase in propane conversion under the typical conditions of 28% propane, 14% oxygen, 2% CO_2, and balance helium with 100 ml/min total flow rate at 600 °C.

3.5. Effect of reaction products on the reaction rates

The reaction pathways were investigated by measuring the influence of product species added to the feed on the reaction rates. Product species were added to the reaction mixture, keeping all the conditions including temperature, partial pressures, and flow rates constant, except for the partial pressure of He to balance the addition. Fig. 8 shows the relation between the amount of CO_2 in the feed and the rates of formation of all products. For the sake of clarity, only the rate of propene formation was plotted on the graph; the rates for the other products can be evaluated via the selectivities. The rates decreased with a negative order in the CO_2 partial pressure as observed in the methane oxidative coupling also [20], while selectivity to propene and ethene was not significantly affected (Fig. 8). The strong inhibition caused by the carbon dioxide appears to be reversible, as the activity was restored to its original value, when CO_2 was removed from the feed.

The influence of the CO_2 concentration on the activity is the most significant effect, whereas all other product species showed only minor effects, as will be shown later. Differential measurements result in correct data only when the

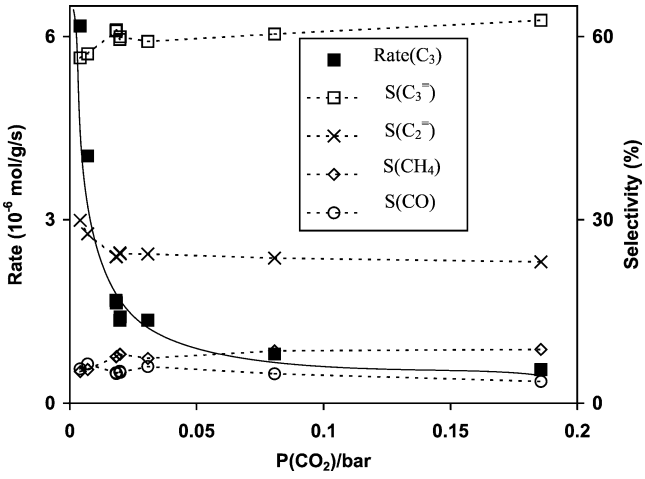

Fig. 8. Influence of CO_2 over catalytic conversion rate of propene and selectivity of the main products. Conditions: $P(C_3H_8)$, 280 mbar; $P(O_2)$, 140 mbar; T, 600 °C; total flow, 100 ml/min; 200 mg catalyst.

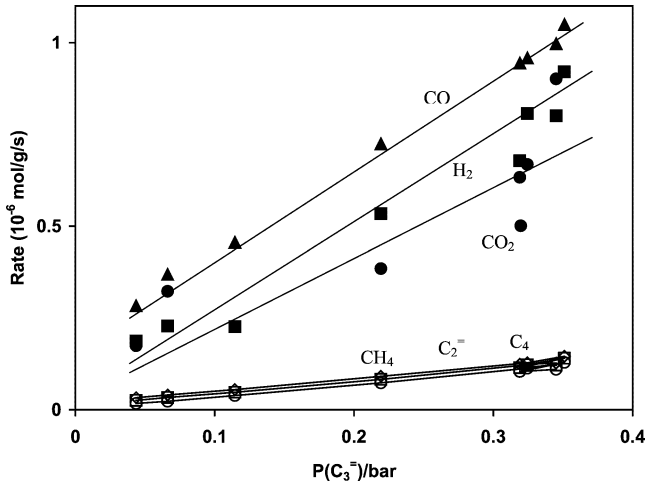

Fig. 9. Propene partial pressure influence over propene conversion. Conditions: $P(CO_2)$, 10 mbar; $P(O_2)$, 70 mbar; T, 600 °C; total flow, 100 ml/min; 200 mg catalyst. CO, triangles; H_2, filled squares; CO_2, filled circles.

concentrations of all species that influence the reaction rates are approximately constant. Therefore, it was necessary to add excess CO_2 to the feed in all differential measurements reported here. Addition of CO_2 to the reaction feed did not have any significant influence upon the reaction rates in the absence of catalyst.

Adding 5% hydrogen to the reaction mixture influenced the reaction rates only to a marginal extent at 600 °C; i.e., the selectivity to CO increased from 9 to 10% and the selectivity to CO_2 decreased from 12 to 11%. Significant conversion of hydrogen was not observed. Addition of water also had no significant influence on the reactions.

The presence CO reduced the reaction rates; however, this inhibiting effect is far smaller than that of CO_2. Adding 5% CO to the reaction stream (which is 10 times more than what is produced in the reaction under the tested conditions) decreased the conversion at 600 °C from 7 to 5% and at 650 °C from 27.5 to 24%. It was observed that part of the CO was converted to CO_2. Selectivities for the major products were not affected significantly.

3.6. Reactions of propene

The rates of formation of products from the primary product propene were measured as a function of the partial pressures of propene, oxygen, and CO_2 in order to assess the reaction kinetics of the secondary reactions. The conditions used were similar to those of propane reaction.

The main products from propene were carbon oxides and hydrogen. The carbon oxides accounted for 70–80% of the products made. Other products included methane, ethene, C_4 (mainly 1-butene), and small amounts of unidentified higher hydrocarbons. The rate of formation of all the measured products varied linearly with the partial pressure of propene (Fig. 9). The rates of formation of methane, ethene, and C_4 were similar over the whole pressure range. The influence of oxygen partial pressure on the propene reaction was clearly

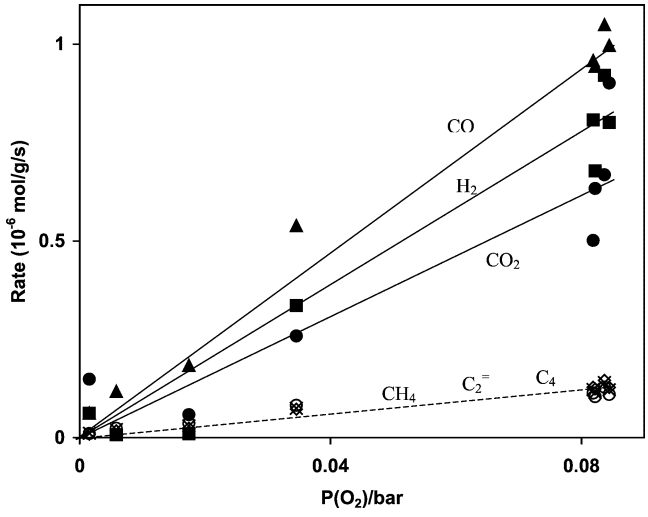

Fig. 10. Oxygen partial pressure effect over propene catalytic oxidation. Conditions: $P(CO_2)$, 10 mbar; $P(C_3H_6)$, 280 mbar; T, 600 °C; total flow, 100 ml/min; 200 mg catalyst. CO, triangles; H_2, filled squares; CO_2, filled circles.

different from its effect on the propane conversion. The rates of formation of the main products noted above increased linearly with oxygen partial pressure (Fig. 10). Also in this case the rates of formation of methane, ethene, and butene varied similarly.

Carbon dioxide had a comparable inhibiting effect on the conversion of propene as on the conversion of propane. Rates of formation of all products decreased with increasing CO_2 partial pressure without markedly changing the product spectrum (Fig. 11). It can be calculated from these data that the reactions to H_2, CO, CO_2, methane, and ethene are order -1 in the CO_2 partial pressure.

Reacting a mixture of propene and hydrogen with oxygen over the catalyst at 600 °C, we did not observe preferential combustion of hydrogen. Adding up to 5 vol% hydrogen

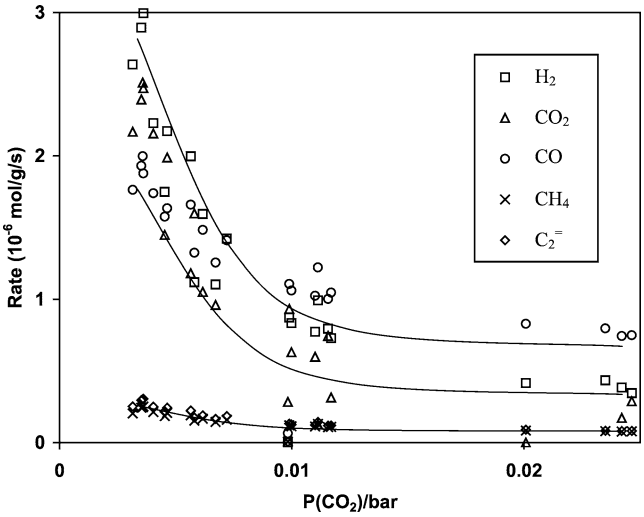

Fig. 11. Influence of CO_2 over the propene oxidative conversion. Conditions: $P(C_3H_6)$, 280 mbar; $P(O_2)$, 70 mbar; T, 600 °C; total flow, 100 ml/min; 200 mg catalyst.

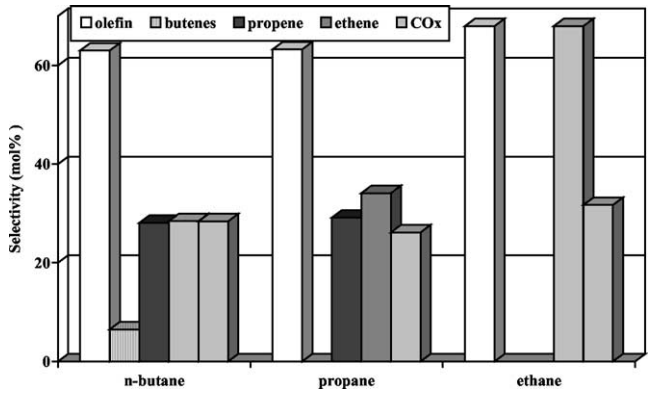

Fig. 12. Selectivities of the main products and hydrocarbon conversion over the Li/Dy/MgO catalyst. Conditions: 6–8% hydrocarbon and 10% oxygen in He; WHSV, 0.8–1/h; T, 650 °C.

did not influence the propene conversion significantly. Upon increasing the hydrogen concentration to 20 vol%, the conversion rate of propene increased by a factor of 2, and the CO formation rate by a factor 2.4. Under these conditions hydrogenation of propene to propane was not observed.

The propene conversion rate was three times lower than the conversion rate of propane over the catalyst under the same experimental conditions (28% hydrocarbon, 7% oxygen, 2% CO_2 at 600 °C). Propene appears to be stable in the gas phase even in the presence of oxygen. The conversion rate of propene was about 40 times lower than the conversion rate of propane under the same conditions (28% hydrocarbon, 7% oxygen at 600 °C).

Addition of 2 vol% propene to the reaction mixture (8 vol% propane and 10 vol% oxygen in He) decreased the conversion of propane by 25–30% over the catalyst at 600 °C. The rate of formation of CO_x from that mixture is equal to the sum of the rates of CO_x formation in the individual reaction of propane and propene. Significant differences in the propene conversion rate were not detected, when it was cofed with propane, compared to oxidation of propene alone.

3.7. Influence of the reactant on the product distribution

In Fig. 12 the selectivities to the main products are shown while using *n*-butane, propane, or ethane as feed under similar conditions. While the conversion level decreased with decreasing carbon chain length of the hydrocarbon, selectivity to total olefins was in the same range in all cases, i.e., between 60 and 70%. Distribution of olefins was rather similar when *n*-butane or propane was the feed; i.e., ethene and propene were produced with similar selectivities, the exception being the small selectivity of butenes from *n*-butane. In the case of ethane the only olefin observed was ethene, as expected. Carbon oxide selectivities were in the same range for all the hydrocarbons.

4. Discussion

4.1. Catalytic vs homogeneous activation of propane

Under certain conditions the conversion in the empty reactor is higher than the conversion in the reactor containing catalyst (see Fig. 13). Therefore we will discuss first the question which of the two routes, homogeneous activation or catalytic activation of propane, prevails in the presence of the catalyst.

Activation of propane takes place predominantly on the catalyst as long as the propane partial pressure is below typically 0.3 bar. This is concluded from the strong inhibiting effect of CO_2 on the catalyst activity at 0.28 bars propane (Fig. 8), while no effect of CO_2 was observed during measurements with the empty reactor. Moreover, a reaction order

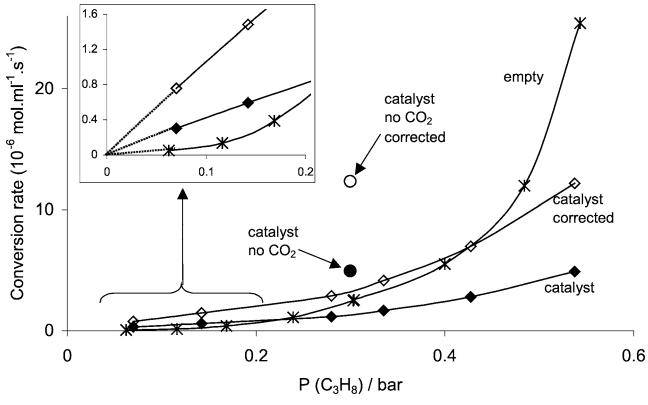

Fig. 13. Volumetric reaction rate of propane conversion vs propane partial pressure: over the catalyst (filled diamonds), over the catalyst corrected for the same residence time as in the empty reactor (open diamonds), and in the empty reactor (stars). Conditions: $P(CO_2)$, 20 mbar, except where noted; $P(O_2)$, 140 mbar; T, 600 °C; total flow, 100 ml/min; 200 mg catalyst or 250 µl cylindrical empty volume.

of one in propane as shown in Fig. 3 clearly differs from the exponential relation observed in the empty reactor (Fig. 5), where the reaction order is continuously increasing with propane partial pressure. Furthermore, Fig. 7 shows a linear relationship between contact time and conversion for the catalyst, whereas the empty reactor shows a sigmoidal relationship. Thus, the activation mechanisms are clearly different in the two cases. The empty reactor shows typical behavior of a radical gas-phase process, during which a pool of radicals needs to be formed to autocatalytically accelerate the reactions [21,22]. In contrast to this, experiments with the catalyst show behavior typical for a catalytic reaction with propane taking part in the rate-determining step. The rates of propane conversion expressed in terms of moles per reactor volume per second with the catalyst and in the empty reactor are compared in Fig. 13. In the same plot, the rate over the catalyst corrected to the same residence time as in the empty reactor, with the dense volume of the catalyst bed, is also shown. In the correction procedure it was assumed that all reactions take place in the volume of the reactor where the catalyst bed is located, and small contributions to the residence time from the entry and exit zones were neglected.

It follows from these observations that the contribution of alkane activation in the gas phase is much smaller when the catalyst is present than in the empty reactor. In Fig. 14 the rates over the catalyst bed (from Fig. 3) are separated into contributions from catalytic activation and homogeneous gas-phase activation. Extrapolating the linear increase at low partial pressures to the high partial pressures, the contribution of the catalyst is tentatively obtained (continuous line in Fig. 14). The second contribution is obtained by subtracting the extrapolated line from the measured data (dashed line in Fig. 14). The resulting curve strongly resembles the dependence of the conversion rate upon propane partial pressure in the empty reactor. Therefore, this contribution is attributed to homogeneous gas-phase reactions. The rate of the homogeneous gas-phase reaction estimated in this way is one order of magnitude lower than the rates observed in the empty reactor. The decrease in contact time caused by the volume occupied by the catalyst cannot account for this decrease. Apparently, quenching of gas-phase radicals takes place similarly to the process observed during methane oxidative coupling [23–26], limiting the formation of a pool of radicals to accelerate the reaction.

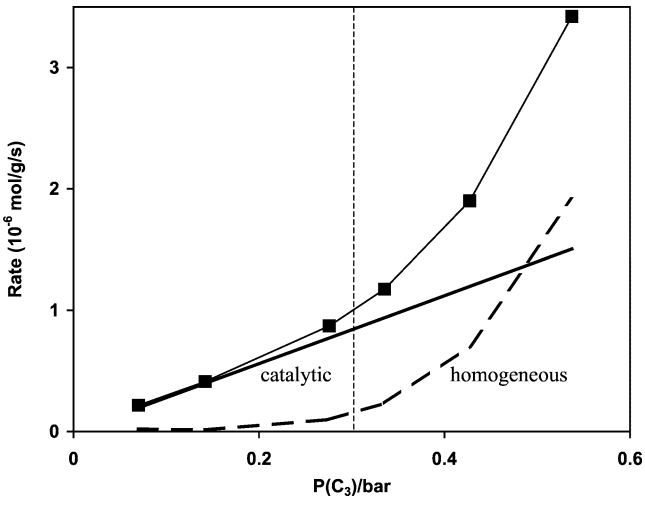

Fig. 14. Decomposition of the rate of propene formation into catalytic and homogeneous contributions. Data from Fig. 3.

In conclusion, it appears that the rate-determining step in the reaction pathways to propene, ethene, and methane involves activation of propane on the catalyst surface, provided that the propane concentration is below typically 0.3 bar, despite the fact that catalyst activity in this study is significantly suppressed by addition of CO_2. Under the typical reaction condition of 28% propane, 14% oxygen, and 2% CO_2, total flow rate of 100 ml/min with the catalyst present, the homogeneous activation is insignificant according to the estimation shown in Fig. 14. However, at the highest propane partial pressure employed (0.5 bar) the contributions of homogeneous gas-phase reactions and catalyzed reactions are approximately equal in the presence of catalyst.

The rate of formation of hydrogen and CO remain linear up to very high propane partial pressures, indicating that these products are mainly formed through catalysis on the solid surface. The comparatively low formation rates of H_2 and CO in the homogeneous reaction support this conclusion.

4.2. The role of oxygen and the reaction mechanism

The role of oxygen in activating propane is complex. The presence of oxygen opens a fast reaction pathway, shown by the marked increase of the rates of hydrocarbon product formation upon increasing the oxygen concentration from 0 to 5 mbar (Fig. 4). This very significant increase is not due to shifting the chemical equilibrium, as the gas composition at the reactor exit is far from the equilibrium even in the absence of oxygen. A stepwise increase of the rates in the empty reactor is also noted (Fig. 6) pointing out the role of gas-phase oxygen in the reaction pathways to the products. However, oxygen does not participate in the rate-determining step at pressures above 5 mbar, as the apparent reaction order in oxygen observed is below 0.2 for propene, ethene, and methane. Oxygen possibly reacts fast with an activated intermediate and this reaction step is rate determining at extremely low oxygen partial pressures only.

The mechanism proposed to be operative under our conditions here is based on homogeneous radical chain propagation reactions, similar to thermal pyrolysis. Thus, we need to introduce the terminology for radical chain reactions. The term “activation” used so far should be understood as “initiation” in the terminology of radical chemistry. We propose that the initiation takes place mainly on the catalyst at low propane partial pressures, while at the highest partial pressures both on the catalysts and in the gas phase. The catalyst influences the radical concentration in two ways, as it not only generates radicals but also quenches them. The place

of initiation is speculated to be a Li^+O^- site [14,17]. Let us examine first the situation without oxygen.

4.3. Mechanism in the absence of gas-phase oxygen

When propane is activated on the catalyst a propyl radical is formed by a hydrogen abstraction. Hydrogen is transferred to the O^- and forms OH^-. In situ DSC studies of methane activation over Li/MgO catalysts at 650 °C showed heat evolution due to surface OH^- formation on the Li^+O^- active site [27]. In situ DRIFTS studies of Li/MgO catalysts under methane oxidative coupling conditions (at 690 °C) showed the presence of strongly bound OH^- [28]. In analogy, we propose that in the presence of catalyst propane will form a propyl radical and surface OH^-. In part II of this publication further evidence will be presented.

Two different propyl radicals can be formed depending on whether primary or secondary hydrogen is abstracted. Based on bond energies we tempt to conclude that predominantly isopropyl radicals are formed on the catalyst (i.e., C–H bond energy on a secondary carbon atom is 3 kcal/mol lower than on the primary one); however, there is no experimental evidence to confirm this. The two radicals have different decomposition routes: *i*-propyl can only undergo β-scission of C–H bonds and decomposes into propene and a hydrogen atom, while *n*-propyl preferentially follows a C–C cleavage in the β position, forming a methyl radical and ethene [29,30]. The methyl radical reacts then with a second propane molecule forming methane and regenerating the propyl radical. The hydrogen atom also reacts with another propane molecule generating a propyl radical, and H_2. The four described reactions are presented below:

$$i\text{-}C_3H_7\cdot \rightarrow C_3H_6 + H\cdot, \quad (1)$$

$$n\text{-}C_3H_7\cdot \rightarrow C_2H_4 + CH_3\cdot, \quad (2)$$

$$CH_3\cdot + C_3H_8 \rightarrow CH_4 + C_3H_7\cdot, \quad (3)$$

$$H\cdot + C_3H_8 \rightarrow H_2 + C_3H_7\cdot. \quad (4)$$

From the kinetic models of the radical chemistry in the oxidative pyrolysis and combustion literature it appears that in the propagation steps, *i*-propyl and *n*-propyl radicals are produced with comparable rates [31–33]. Consequently rates of reactions (1) and (2) should be similar, and the same follows for rates of reactions (3) and (4). Thus, formally the probability of C–C and C–H bond breakage is comparable. This would result in a similar amount of propene, ethene, methane, and hydrogen, which agrees well with our experimental observations at very low oxygen partial pressures (points at 0 bar oxygen in Fig. 4 and Fig. 6). Similar ratios between the products were also observed in thermal cracking (without oxygen) at low conversions [31,34].

4.4. Mechanism in the presence of gas-phase oxygen

The presence of oxygen has two important effects. First, we discuss the influence of oxygen on the homogeneous chemistry that takes place. Second, we will discuss the effect of oxygen on the catalyst.

The enhancement seen by the oxygen addition can also be explained with the proposed radical chemistry [35]. The introduction of oxygen, even in small amounts, increases the number and the concentration of the chain carrier radicals. When oxygen is not present $H\cdot$ and $\cdot CH_3$ radicals are the main chain propagators according to reactions (1)–(4). In the presence of oxygen the *i*-propyl radical reacts fast with the oxygen molecule forming a hydroperoxyl ($HO_2\cdot$) radical and propene. The hydroperoxyl radical further reacts with a new propane molecule forming H_2O_2, which by decomposition gives two hydroxyl radicals ($\cdot OH$). $\cdot OH$ becomes the main chain propagator [36] and it forms water by reacting with a propane molecule. This is perfectly in line with the fact that hydrogen combustion did not occur selectively in our reactor. Thus, we conclude that water is mainly formed in the above-described process. The similarity of the influence of small amount of oxygen on the propane conversion in the absence and presence of catalyst confirms the proposal that O_2 mainly influences the gas-phase radical propagation reactions, independent of the origin of radical initiation.

The $CH_3\cdot$ radical is the precursor for CO and CH_4 in the presence of oxygen. When ethene is formed through reaction (2) a methyl radical is produced that can react further either to methane or CO. If this methyl radical reacts with a propane molecule, methane is formed. If it reacts with oxygen an oxygenated intermediate is formed, which is subsequently transformed into CO and further to CO_2. Because the same numbers of $CH_3\cdot$ radicals and ethene molecules are formed in reaction (2) the sum of the formation rates of CH_4 and CO equals the formation rate of ethene over the whole range of partial pressures of both propane and oxygen (see Figs. 3 and 4). In the empty reactor the sum of the rates of CO and CH_4 formation does not match the ethene formation rate. We speculate therefore that a stable oxygen-containing C_1 intermediate is formed (formaldehyde, for example) which is quantitatively converted to CO over the catalyst, but is stable in the gas phase. Analysis of oxygenates was not performed, but the small gap in the carbon balance (2–3%) makes this hypothesis feasible, since mechanistic models of homogeneous alkane oxidation predict the formation of formaldehyde [23,36].

So far we have dealt with hydrocarbon activation and gas-phase reaction steps. The proposed reaction mechanism is schematically represented in Fig. 15. Assuming the proposed initiation on the catalyst by hydrogen abstraction, the question arises as to how the catalytic sequence is closed by regeneration of the active site, i.e., how hydrogen is removed from the active oxygen.

In the methane oxidative coupling literature primarily Li/MgO dehydroxylation was proposed as the regeneration step [37]. However, this step requires an energetically demanding removal of lattice oxygen. Regeneration of the active site is possible without dehydroxylation with the help of O_2. Recently a new mechanism has been proposed that

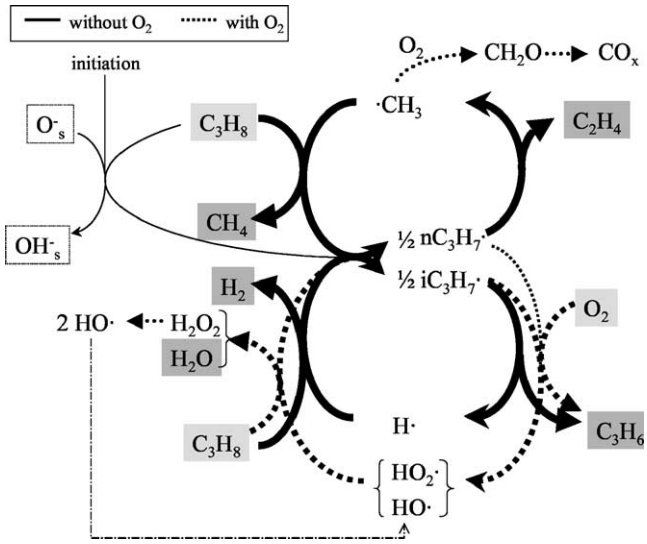

Fig. 15. The scheme of the proposed reaction mechanism.

does not require the highly energetic removal of lattice oxygen, based on computation of energetic state of various surface intermediates [38]. A sequence of reactions has been proposed by Sinev et al. [39,40]. The four reactions proposed are presented below:

$$O_2 + OH_s^- \rightarrow O_s^- + HO_2\cdot, \quad (5)$$

$$HO_2\cdot + OH_s^- \rightarrow O_s^- + H_2O_2, \quad (6)$$

$$H_2O_2 \rightarrow 2\cdot OH, \quad (7)$$

$$\cdot OH + OH_s^- \rightarrow O_s^- + H_2O. \quad (8)$$

The overall reaction equation of the regeneration is the same as in the mechanism proposed by Ito et al. [37] but it does not require or suggest the removal of lattice oxygen. The experimental demonstration of this mechanism at 650 °C showed that OH_s^- is decomposed upon admission of oxygen to the reactor while water is formed [39,40]. It was also shown that dehydroxylation can occur as well especially at high temperatures as a parallel regeneration route [41]. Analysis of the literature data on redox mode methane coupling suggests that at intermediate temperatures (600–650 °C) regeneration must occur without lattice oxygen removal, while at high temperatures (> 700 °C) lattice oxygen removal is the most feasible route [42,43]. In addition to water elimination by dehydroxylation, some dihydrogen elimination from the Li/MgO catalyst was also reported above 600 °C [44]. The prevailing route under our conditions is, therefore, speculated to be the mechanism described in Eqs. (5)–(8).

4.5. Effects of by-products on the catalytic performance

CO_2 inhibits the reaction by adsorbing at the active Li^+O^- site. It has been shown earlier, that these types of catalysts strongly adsorb CO_2. TPD of carbon dioxide suggested that Li_2CO_3 forms under reaction conditions [14]. The fact that selectivities do not change upon CO_2 addition (Fig. 8) is in agreement with the hypothesis that the conversion of propyl radicals to propene, ethene, and methane is controlled by gas-phase reactions, which are not influenced by CO_2. Fitting the rate data (only the catalytic contribution) results in a -1 order in CO_2 partial pressure. It is speculated that Li_2CO_3 is not formed directly, as that would result in -0.5 order, but possibly a stable precursor is formed initially. Adsorbing CO_2 on the Li^+O^- site results in $Li^+CO_3^-$ [45], which indeed has been detected by ESR [46]. Adsorbed CO_2 was also detected by in situ IR spectroscopy, and it was suggested that CO_3^- formed is precursor for carbonate formation [28]. An alternative, though similar, explanation for the -1 order in CO_2 is based on the suggestion that under reaction conditions a large fraction of the active Li^+O^- sites exist in the form of Li^+OH^- [47]. Reaction of Li^+OH^- with CO_2 would result in lithium bicarbonate, accounting for the -1 order.

The small inhibiting effect of CO is tentatively explained by slow transformation of CO to CO_2 that subsequently blocks the active site possibly without desorption.

4.6. Importance of secondary reactions

It has been shown earlier that the rate of conversion of propene was a factor 3 lower than the corresponding rate of propane conversion under the same conditions when catalyst was used [17]. Propene appears to be even more stable in the gas phase, because propene conversion was 40 times lower than propane conversion under similar conditions, when an empty reactor was used. Thus, we conclude that propene conversion occurs through catalytic reactions. This is also in agreement with the observation that CO_2 inhibits the conversion of propene (Fig. 11). Moreover, the CO_2 inhibition also suggests that the catalytic site for propene activation must be the same Li^+O^- active center as for propane activation.

The remarkable stability of propene in the gas phase can be explained by the stability of the allyl ($C_3H_5\cdot$) radical, which is formed upon activation of propene. The part of reaction pathways, which occurs in the gas phase, depends on the reactivity of the radicals released upon activation. Allyl radicals do not have a fast decomposition route in the gas phase, unlike the propyl radicals that are considerably more reactive. Therefore, the efficiency of propagation steps is greatly reduced; consequently, propane conversion due to radical chain propagation reactions is higher than that of propene [48].

CO_x forms on the catalyst in analogous mode from propane and propene, as follows. CO is formed from propane only through catalytic activation pointed out by the first order in propane for the whole partial pressure range (Fig. 3) and the absence of any formation of CO in the empty reactor at propane pressure below 0.3 bar (Fig. 5), while CO formation was rate limited in oxygen (0.5 order in Fig. 4). Similarly, Figs. 9, 10 show that the conversion of propene to CO and CO_2 is first order in both propene and oxygen. This

suggests a rate-determining step involving both propene and oxygen. Note, that the rate of CO_x formation is comparable from both hydrocarbons; thus the total oxidation of propane at low conversions, during differential measurements in this paper, does not significantly occur via the consecutive reaction of propene.

The presence of propane does not seem to influence the conversion of propene significantly, but the conversion of propane is reduced if propene is present, probably by "quenching" of the radicals by the propene molecule while forming less reactive allyl radical.

The enhancement of propene conversion upon addition of hydrogen can be explained by the fact that hydrogen removes the carbonate from the surface of the catalyst, as we observed some CO evolution when hydrogen was fed over the catalyst in the absence of any significant hydrogen conversion. In this manner hydrogen increases the availability of active sites, and thus contributes to the enhancement of the reaction.

4.7. C–C vs C–H bond breaking

Special attention will be paid to cleavage of C–H bonds versus cleavage of C–C bonds as these steps control the selectivity to propene and ethene, respectively. The mechanism proposed above describes the conversion of propane as heterogeneously initiated chain propagation reactions in the gas phase. Initiation over the catalyst prevails as long as the propane partial pressure is below typically 0.3 bar. In this mechanism the product distribution is mainly determined by the gas-phase propagation steps. New experimental evidence provides additional support for this hypothesis.

The decrease of dehydrogenation selectivity and increase of cracking selectivity with temperature over Li/MgO (Fig. 1) are explained by the higher activation energy of formation of the primary alkyl radicals in the propagation reactions [23]. The primary radicals preferably follow a decomposition route involving C–C bond breakage.

The fact that the activity observed for ethane is significantly different from that for propane and butane (Fig. 12) supports the proposition that the rate-determining step is hydrogen abstraction, i.e., a C–H bond breakage, during both catalytic initiation and gas-phase propagation. The bond energy of a secondary C–H bond is similarly the weakest in propane and butane (98.5 and 98.2 kcal/mol, respectively), while a primary C–H bond energy is somewhat higher in all the alkanes (101.1 kcal/mol) [49,50]. Since ethane possesses only primary C–H bonds, its activity is significantly different from propane and butane, as the alkane conversion is determined by the rate of C–H bond scission.

The distribution of olefins formed from ethane, propane, and butane can be explained by the decomposition routes of the radicals according to the homogeneous radical chemistry [23,51]. A primary radical, whether propyl or butyl, leads preferentially to C–C bond cleavage in β position, resulting in cracked products, except for the ethyl radical which can only brake a C–H bond in β position. A secondary propyl radical can only break a C–H bond resulting in propene, while a secondary butyl radical can lead to either C–C or C–H bond cleavage, resulting in propene or butene production. It follows that more cracked products are expected from butane than from propane, and hardly any cracking from ethane, which is indeed observed experimentally (Fig. 12).

Secondary reactions of propene proceed with a much lower rate than the primary reactions. This follows from the observation that the conversion level of propane does not influence the selectivities (Fig. 2), unlike in the case of typical redox catalysts such as vanadia [5,52]. This is in line with the observations that propene conversion is a factor of 3 lower than that of propane under similar conditions, and is attributed to the relatively low reactivity of allyl radicals in the gas phase.

5. Conclusions

In this paper the main features of the reaction kinetics of the oxidation of propane and propene over Li/Dy/MgO catalysts have been described. A mechanism that qualitatively explains these kinetic results is proposed in terms of mixed heterogeneous–homogeneous radical reaction routes.

Alkane activation via a C–H bond splitting is the rate-determining step for all reaction products. For propane, rates are first order up to 0.3 bar propane. At high propane partial pressures (> 0.3 bar) the reaction order increases for all hydrocarbon products. This has been attributed to contributions from homogeneous activation of propane.

The presence of gas-phase oxygen appears to be crucial for propane conversion. The strong increase of the reaction rates by increasing the oxygen concentration has been attributed to the interaction of oxygen molecules with the chain-carrier radicals, opening a fast reaction pathway via OH radicals. A second function of oxygen is to regenerate the catalyst via removal of hydrogen from the catalyst in order to restore the activity of the catalyst for generation of radicals.

Carbon dioxide strongly suppresses the activity of the catalyst for all products. The apparent order is -1, which is attributed to blocking of active sites by forming $Li^+CO_3^-$ on the active site. Reactions in the gas phase were not influenced by CO_2.

Consecutive reactions of propene give almost exclusively carbon oxides and proceeds mainly on the catalyst. The rate of conversion is low compared to the rate of conversion of propane due to the relative stability of the intermediate allyl radical compared to the propyl radical under reaction conditions.

The conversion trends of ethane, propane, and butane confirm that hydrogen abstraction from the alkane is the rate-determining step. Gas-phase radical chemistry determines largely the selectivity pattern.

Acknowledgments

This work was performed under the auspices of The Netherlands Institute for Catalysis Research (NIOK) and the Process-Technology Institute Twente (PIT). The financial support from STW Project No. 349-4428 is gratefully acknowledged. L. Leveles is grateful to Dipl.-Ing. U. Kürten for helpful discussions regarding the mechanism.

References

[1] R.K. Grasselli, D.L. Stern, J.G. Tsikoyiannis, Appl. Catal. A: Gen. 189 (1999) 1.
[2] F. Nierlich, Hydrocarbon Proc. 71 (1992) 45.
[3] Petrochemistry activity review http://www.cefic.org, 1999–2000.
[4] M.M. Bhasin, J.H. Mccain, B.V. Vora, T. Imai, P.R. Pujado, Appl. Catal. A: Gen. 221 (2001) 397.
[5] S. Albonetti, F. Cavani, F. Trifiro, Catal. Rev.-Sci. Eng. 38 (1996) 413.
[6] F. Cavani, F. Trifiro, Catal.Today 24 (1995) 307.
[7] H.H. Kung, Adv. Catal. 40 (1994) 1.
[8] F. Cavani, F. Trifiro, Catal. Today 36 (1997) 431.
[9] M.V. Landau, M.L. Kaliya, M. Herskowitz, P.F. van den Oosterkamp, P.S.G. Bocque, Chemtech 26 (1996) 24.
[10] M.V. Landau, M.L. Kaliya, A. Gutman, L.O. Kogan, M. Herskowitz, P.F. van den Oosterkamp, Stud. Surf. Sci. Catal. 110 (1997) 315.
[11] S.J. Conway, J.H. Lunsford, J. Catal. 131 (1991) 513.
[12] S.J. Conway, D.J. Wang, J.H. Lunsford, Appl. Catal. A 79 (1991) L1–L5.
[13] M.A. Banares, Catal. Today 51 (1999) 319.
[14] M.Y. Sinev, V.Y. Bychkov, V.N. Korchak, O.V. Krylov, Catal. Today 6 (1990) 543.
[15] R. Burch, E.M. Crabb, Appl. Catal. A 100 (1993) 111.
[16] M. Xu, J.H. Lunsford, React. Kinet. Catal. Lett. 57 (1996) 3.
[17] L. Leveles, S. Fuchs, K. Seshan, J.A. Lercher, L. Lefferts, Appl. Catal. A: Gen. 227 (2002) 287.
[18] D.E. Mears, J. Catal. 20 (1971) 127.
[19] D.E. Mears, Chem. Eng. Sci. 26 (1971) 1361.
[20] J.A. Roos, S.J. Korf, R.H.J. Veehof, J.G. van Ommen, J.R.H. Ross, Appl. Catal. 52 (1989) 131.
[21] A. Beretta, E. Ranzi, P. Forzatti, Chem. Eng. Sci. 56 (2001) 779.
[22] M.C. Huff, I.P. Androulakis, J.H. Sinfelt, S.C. Reyes, J. Catal. 191 (2000) 46.
[23] C.A. Mims, R. Mauti, A.M. Dean, K.D. Rose, J. Phys. Chem. 98 (1994) 13357.
[24] P.M. Couwenberg, Q. Chen, G.B. Marin, Ind. Eng. Chem. Res. 35 (1996) 3999.
[25] M. Hatano, P.G. Hinson, K.S. Vines, J.H. Lunsford, J. Catal. 124 (1990) 557.
[26] M.H. Back, R. Martin, Int. J. Chem. Kin. 11 (1979) 757.
[27] V.Y. Bychkov, M.Y. Sinev, V.N. Korchak, E.L. Aptekar, O.V. Krylov, Kinet. Catal. 30 (1989) 989.
[28] S.C. Bhumkar, L.L. Lobban, Ind. Eng. Chem. Res. 31 (1992) 1856.
[29] N. Yamauchi, A. Miyoshi, K. Kosaka, M. Koshi, N. Matsui, J. Phys. Chem. A 103 (1999) 2723.
[30] L.C. Jitariu, F. Wang, I.H. Hillier, M.J. Pilling, Phys. Chem. Chem. Phys. 3 (2001) 2459.
[31] D. Perrin, R. Martin, Int. J. Chem. Kinet. 32 (2000) 340.
[32] C.K. Westbrook, W.J. Pitz, Combust. Sci. Technol. 37 (1984) 117.
[33] W. Tsang, J. Phys. Chem. Ref. Data 17 (1988) 887.
[34] P.S. Van Damme, S. Narayanan, G.F. Froment, AIChE J. 21 (1975) 1065.
[35] V.R. Choudhary, V.H. Rane, A.M. Rajput, AIChE J. 44 (1998) 2293.
[36] A. Beretta, P. Forzatti, E. Ranzi, J. Catal. 184 (1999) 469.
[37] D.J. Driscoll, W. Martir, J.X. Wang, J.H. Lunsford, Adv. Catal. 35 (1987) 139.
[38] M.A. Johnson, E.V. Stefanovich, T.N. Truong, J. Phys. Chem. B 101 (1997) 3196.
[39] M.Y. Sinev, V.Y. Bychkov, Kinet. Katal. 34 (1993) 309.
[40] M.Y. Sinev, V.Y. Bychkov, V.N. Korchak, E.L. Aptekar, O.V. Krylov, Kinet. Catal. 30 (1989) 1236.
[41] M.Y. Sinev, V.Y. Bychkov, Kinet. Catal. 34 (1993) 272.
[42] V.R. Choudhary, V.H. Rane, S.T. Chaudhari, React. Kinet. Catal. Lett. 63 (1998) 371.
[43] G.C. Hoogendam, PhD thesis, University of Twente, The Netherlands, 1996.
[44] T. Karasuda, K. Aika, J. Catal. 171 (1997) 439.
[45] M. Che, A.J. Tench, Adv. Catal. 31 (1982) 77.
[46] N.G. Maksimov, G.E. Selyutin, A.G. Anshits, E.V. Kondratenko, V.G. Roguleva, Catal. Today 42 (1998) 279.
[47] M.Y. Sinev, Catal. Today 24 (1995) 389.
[48] A.A. Konnov, 2000. Detailed reaction mechanism for small hydrocarbons combustion. Release 0.5. Webpage, http://homepages.vub.ac.be/~akonnov/.
[49] M.L. Poutsma, J. Anal. Appl. Pyrolysis 54 (2000) 5.
[50] J. Berkowitz, G.B. Ellison, D. Gutman, J. Phys. Chem. 98 (1994) 2744.
[51] E. Ranzi, A. Sogaro, P. Gaffuri, G. Pennati, C.K. Westbrook, W.J. Pitz, Combust. Flame 99 (1994) 201.
[52] H.H. Kung, M.C. Kung, Appl. Catal. A 157 (1997) 105.